

7.1 Introduction

Physical properties of individual mesogens may or may not undergo modifications in their mixtures. Sometimes, the modifications become characteristic thereby making the study of mixtures important. Earlier studies [311, 316, 317-319, 321, 324, 493-498] have suggested the formation of mixed mesomorphism by mixing compounds where none, one, or both of them are mesogens. Most of the binary mixtures do not undergo any change in their mesomorphic textures, though a few have been reported giving rise to different textures [317]. Emergence of the mesophase, increase or decrease of the mixed mesomorphic ranges and thermal stabilities, and the study of the factors that influence the modification have received more attention [317,324, 496-501]. Our group has reported mixtures where a higher-order smectic phase emerges from binary mixtures of nematogens and a lower-order nematic phase emerges from a binary mixture of a smectogen [321] and a non-mesogen. Binary systems of structurally similar and dissimilar mesogens and non-mesogens [318] have also been studied and reported. Keeping this in view, we report here ten binary systems consisting of part I binary systems of mesogens with non-mesogenic and mesogenic carboxy esters. Part II consists of six binary systems of chiral dopant in different types of mesogenic and non-mesogenic components.

Binary systems

Type 1: Components

A1 = 4-(4'-*n*-butoxybenzoyloxy) 3-methylphenyl azo-2'', 4''-dimethylbenzene [**BBMPAD**]

A2 = 4-(4'-*n*-hexyloxybenzoyloxy) 3-methylphenyl azo-2'', 4''-dimethylbenzene [**HBMPAD**]

B1 = 4-nitrophenyl-4-*n*-butoxybenzoate [**NPBB**]

B2 = 4-nitrophenyl-4-*n*-hexyloxybenzoate [**NPHB**]

Type 2: Components

X1 = 4-(4'-*n*-octyloxycinnamoyloxy)-phenylazo-2'', 4''-dimethylbenzene [**8CiXYP**]

X2 = 1-methoxy-4-[(4-methoxyphenyl)-NNO-azoxy] benzene (p-azoxyanisole) [**PAA**]

X3 = N-(4-methoxybenzylidene)-4-nitrobenzenamine [**MSN**]

X4 = 4-butoxybenzoic acid [**4ABA**]

X5 = 3-(4-butoxyphenyl)-propenoic acid [**4ACA**]

X6 = 4'-*n*-heptyloxy quinolin-8-yl-benzoate [**7HQE**]

Y = Cholesteryl-4-nitrobenzoate [**CHOLN**]

7.2 Experimental

7.2.1 Materials

(1) 4-nitro phenol, (2) 8-hydroxy quinoline, (3) Cholesterol, (4) 4-methylaniline, (5) 4-nitrobenzaldehyde (6) p- azoxyanisole all the chemicals are of Merck or Loba grade and are used as received.

7.2.2 Synthesis

7.2.2.1 Component A1

Component A1 is synthesized following the procedure reported and described in 3.2.2.1b and 3.2.2.2d [433, 440].

FTIR (KBr pellets, cm^{-1}): 2954 – 2858 (–C–H St, Alkyl CH_3 , SP^3 hybridization), 1733 (–C=O– St. of ester), 1604 (–N=N– St.), 1574 – 1505 (–C=C– St. of Aromatic ring), 1482(–C–H bending of – CH_2 –), 1248(Aromatic ether St.), 1067(–C–O– St. of ester), 895(strong –C–H– bending for 1:2:4 tri substituted benzene ring), 725 (weak –C–H– bending for – $(\text{CH}_2)_{11}$ –).

7.2.2.2 Component A2

Component A1 is synthesized following the procedure reported described in 3.2.2.1b and 3.2.2.2d [433, 440].

FTIR (KBr pellets, cm^{-1}): 2954 – 2858 (–C–H St, Alkyl CH_3 , SP^3 hybridization), 1733 (–C=O– St. of ester), 1604 (–N=N– St.), 1574 – 1505 (–C=C– St. of Aromatic ring), 1482(–C–H bending of – CH_2 –), 1248(Aromatic ether St.), 1067(–C–O– St. of ester), 895(strong –C–H– bending for 1:2:4 tri substituted benzene ring), 725 (weak –C–H– bending for – $(\text{CH}_2)_{11}$ –).

7.2.2.3 Component B1

Component B1 is synthesized following the procedure reported and described in 3.2.2.1b and 3.2.2.2d [433, 440]

FTIR (KBr pellets, cm^{-1}): 2954 – 2858 (–C–H St, Alkyl CH_3 , SP^3 hybridization), 1733 (–C=O– St. of ester), 1574 – 1505 (–C=C– St. of Aromatic ring), 1520(Asymmetric aromatic – NO_2), 1345(Symmetric aromatic – NO_2), 1482(–C–H bending of – CH_2 –), 1248(Aromatic ether St.), 1067(–C–O– St. of ester), 895(strong –C–H– bending for 1:2:4 tri substituted benzene ring), 725 (weak –C–H– bending for – $(\text{CH}_2)_{11}$ –).

7.2.2.4 Component B2

Component B2 is synthesized following the procedure reported and described in 3.2.2.1b and 3.2.2.2d [433, 440].

FTIR (KBr pellets, cm^{-1}): 2954 – 2858 (–C–H St, Alkyl CH_3 , SP^3 hybridization), 1733 (–C=O– St. of ester), 1574 – 1505 (–C=C– St. of Aromatic ring), 1520(Asymmetric aromatic – NO_2), 1345(Symmetric aromatic – NO_2), 1482(–C–H bending of – CH_2 –), 1248(Aromatic ether St.), 1067(–C–O– St. of ester),

895 (strong -C-H- bending for 1:2:4 tri substituted benzene ring), 725 (weak -C-H- bending for $\text{-(CH}_2\text{)}_{11}\text{-}$).

7.2.2.5 Component X1

Component X1 is synthesized following the procedure reported in 3.2.2.4d [440].

FTIR (KBr pellets, cm^{-1}): 2935–2860 cm^{-1} (-C-H , stretching, alkyl -CH_3 , sp^3 hybridization), 1735 cm^{-1} (-C=O stretching of ester), 1630 cm^{-1} (-C=C- , stretching, Vinyl group of cinnamate), 1604 cm^{-1} (-N=N- stretching), 1515–1475 cm^{-1} (-C=C- stretching of aromatic ring), 1450 cm^{-1} (-C-H bending of -CH_2), 1180 cm^{-1} (-C-O stretching ester, sp^2 hybridization), 840 cm^{-1} (-C-H bending of 1,4-disubstituted benzene ring), 720 cm^{-1} (weak -C-H bending for $\text{-(CH}_2\text{)}_n\text{-}$).

7.2.2.6 Component X2

Component X2 is used as received.

7.2.2.7 Component X3

Component X3 is synthesized following the procedure reported in 4.2.2.1c [453].

FTIR (KBr pellets, cm^{-1}): 2935–2860 (-C-H , stretching, alkyl -CH_3 , sp^3 hybridization), 1735 (-C=O stretching of ester), 1630 (-C=C- , stretching, Vinyl group of cinnamate), 1604 (-C-H st. of -C=N-), 1515–1475 (-C=C- stretching of aromatic ring), 1450 (-C-H bending of -CH_2), 1180 (-C-O stretching ester, sp^2 hybridization), 840 (-C-H bending of 1,4-disubstituted benzene ring), 720 (weak -C-H bending for $\text{-(CH}_2\text{)}_n\text{-}$).

7.2.2.8 Component X4

Component X4 is synthesized following the procedure reported in 3.2.2.1a [433].

FTIR (KBr pellets, cm^{-1}): 2935–2860 (-C-H , st., alkyl -CH_3 , sp^3 hybridization), 2935 (-O-H st. of Acid), 1515–1475 (-C=C- st. of aromatic ring), 1450 (-C-H bending of -CH_2), 840 (-C-H bending of 1,4-disubstituted benzene ring), 720 (weak -C-H bending for $\text{-(CH}_2\text{)}_n\text{-}$).

7.2.2.9 Component X5

Component X5 is synthesized following the procedure reported in 3.2.2.4b [439].

FTIR (KBr pellets, cm^{-1}): 2935–2860 (-C-H , st., alkyl -CH_3 , sp^3 hybridization), 2935 (-O-H st. of acid), 1630 (-C=C- , st. Ar-CH), 1515–1475 (-C=C- st. of aromatic ring), 1450 (-C-H bending of $\text{-CH}_2\text{-}$), 1180

(–C–O st. ester, sp^2 hybridization), 840 (–C–H bending of 1,4-disubstituted benzene ring), 720 (weak –C–H bending for $-(CH_2)_n-$).

7.2.2.10 Component X6

Component X6 is synthesized following the procedure reported in 3.2.2.4d [440].

FTIR (KBr pellets, cm^{-1}): 2930–2858 (–C–H, st., alkyl CH_3 , sp^3 hybridization), 1735 (–C=O st. of ester), 1635 (–C=C–, st., Vinyl group of cinnamate), 1515–1475 (–C=C– stretching of aromatic ring), 1450 (–C–H bending of $-CH_2-$), 1180 (–C–O st. ester, sp^2 hybridization), 842 (–C–H bending of 1,4-disubstituted benzene ring), 724 (weak –C–H bending for $-(CH_2)_n-$).

7.2.2.11 Component Y

Component Y is synthesized following the procedure reported in 3.2.2.4d [440].

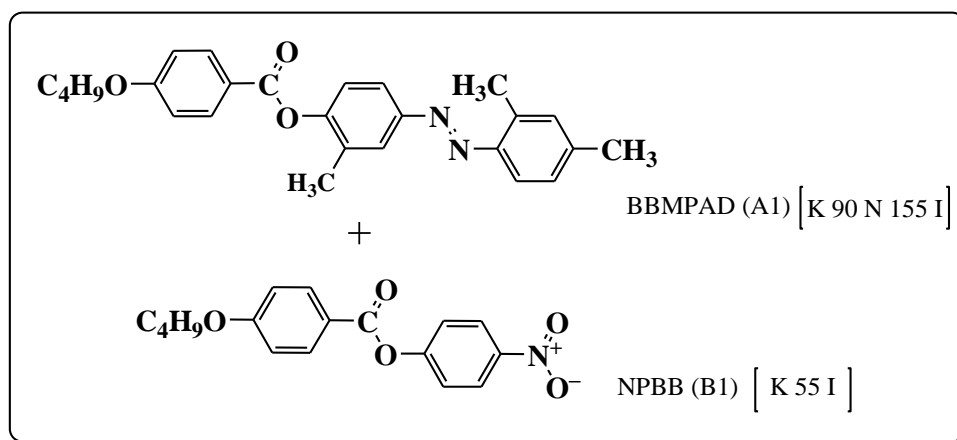
FTIR (KBr pellets, cm^{-1}): 2952–2858 (–C–H st., Alkyl $-CH_3$, sp^3 hybridization), 1750 (–C=O ester), 1579–1508 (–C=C st. aromatic ring), 1480 (–C–H bending of $-CH_2-$), 860 (–CH=CH– st.), 1069 (–C–O st. ester), 860–850 (Para-substituted phenyl ring), 1520 (Asymmetric aromatic $-NO_2$), 1345 (Symmetric aromatic $-NO_2$).

7.2.3 Preparation and study of binary mixtures

The components were weighed in known proportions and melted together in fusion tubes. They were thoroughly mixed in their melt to obtain a homogeneous mixture, after which they were cooled. This procedure was repeated three to four times. The solid obtained was finally ground and used for determining transition temperatures, by using a Leitz Laborlux 12 POL polarizing microscope fitted with a Kofler heating stage.

7.3 Type 1 Binary System [I to VI]

7.3.1 Binary System I: BBMPAD (A1) + NPBB (B1)



In this system (Table 7.1, Figure 7.1) the ester component B1 is non-mesomorphic in nature (K 55 I); whereas the azo-ester mesogen A1 is mesomorphic in nature (K 90 N 155 I) exhibiting nematic phase with Schlieren texture. The mesogenic characteristic commences in the form of enantiotropic nematic with the addition of as low as 7.74 mole % of A1 component to B1 and it continues to be exhibited till the last binary mixture studied. The binary System shows threaded/marble texture of nematic phase. The N-I curve shows deviation from linearity. The maximum mesophase range of 76°C is obtained at 63.85 mole% of A1. Eutectic point is obtained at 53.19 mole % of A1 with eutectic temperature 45 °C and mesophase range of 70 °C at this point.

Table 7.1: Binary System I: BBMPAD (A1) + NPBB (B1)

MOLE % OF A1	TRANSITION TEMPERATURE (NEMATIC °C)	TRANSITION TEMPERATURE (ISOTROPIC °C)
0.00	-	55
7.74	49	58
15.89	51	70
24.49	55	85
33.54	52	88
43.07	46	94
53.19	45	115
63.85	52	128
75.20	62	134
87.21	80	143
100.00	90	155

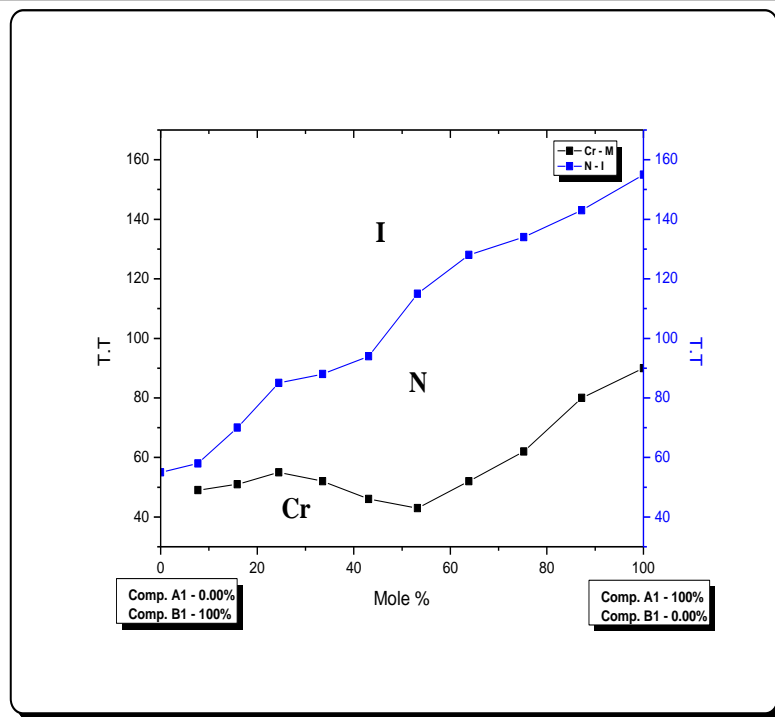
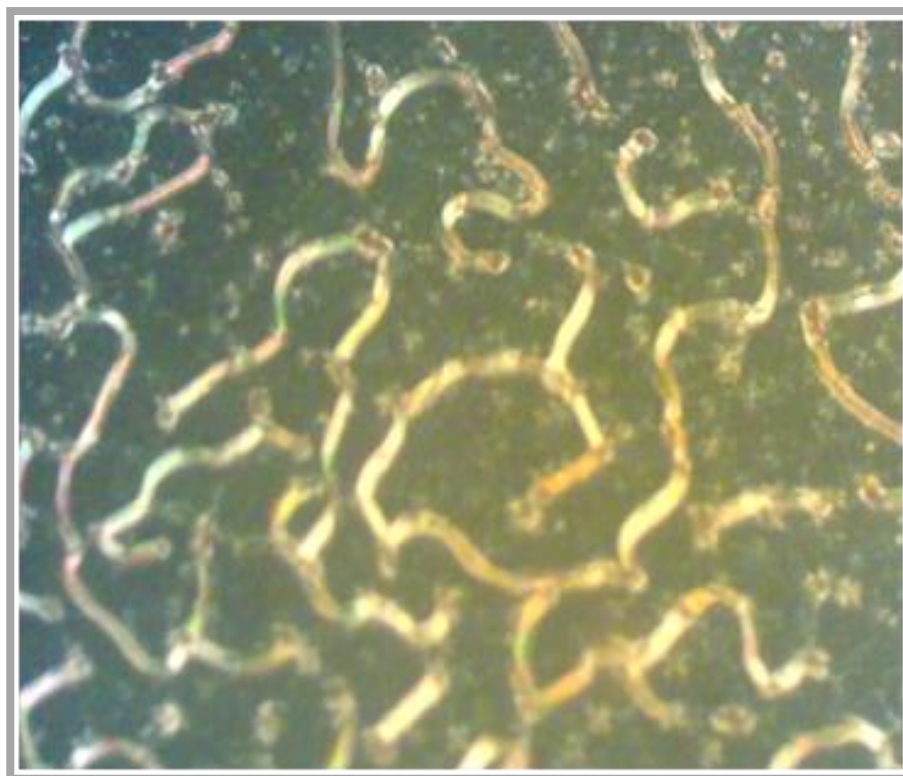


Figure 7.1: Phase diagram of Binary System I: BBMPAD (A1) + NPBB (B1)

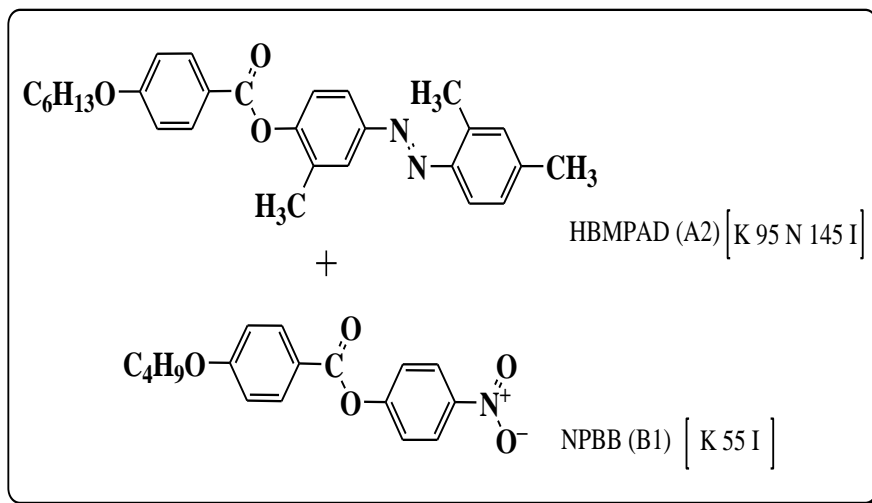
Polarizing optical microscopic image of Liquid Crystal

Polarizing optical microscopic image of binary system I at 53.19 mole%



Threaded texture of nematic phase of binary system I at 53.19 mole% at 101 °C on cooling.

7.3.2 Binary system II: HBMPAD (A2) + NPBB (B1)



In this system (Table 7.2, Figure 7.2) the ester component B1 is non-mesomorphic in nature (K 55 I); whereas the azo mesogen A2 is mesomorphic in nature (K 95 N 145 I) exhibiting enantiotropic nematic phase with Schlieren texture. The mesogenic characteristic commences in enantiotropic nematic form with the addition of as low as 7.30 mole % of A2 component and it continues to be exhibited till the last binary mixture studied. The eutectic point is sharp and obtained at 38 °C with 51.54 mole % of A2. The N-I curve shows deviation from linearity and highest mesophase range of 76 °C is obtained at 62.30 mole% of A2.

Table 7.2: Binary System II: HBMPAD (A2) + NPBB (B1)

MOLE % OF A2	TRANSITION TEMPERATURE (NEMATIC °C)	TRANSITION TEMPERATURE (ISOTROPIC °C)
0.00	-	55
7.30	52	65
15.05	51	76
23.31	55	81
32.09	50	88
41.37	47	91
51.54	38	96
62.30	55	131
73.96	63	132
86.47	84	141
100.00	95	145

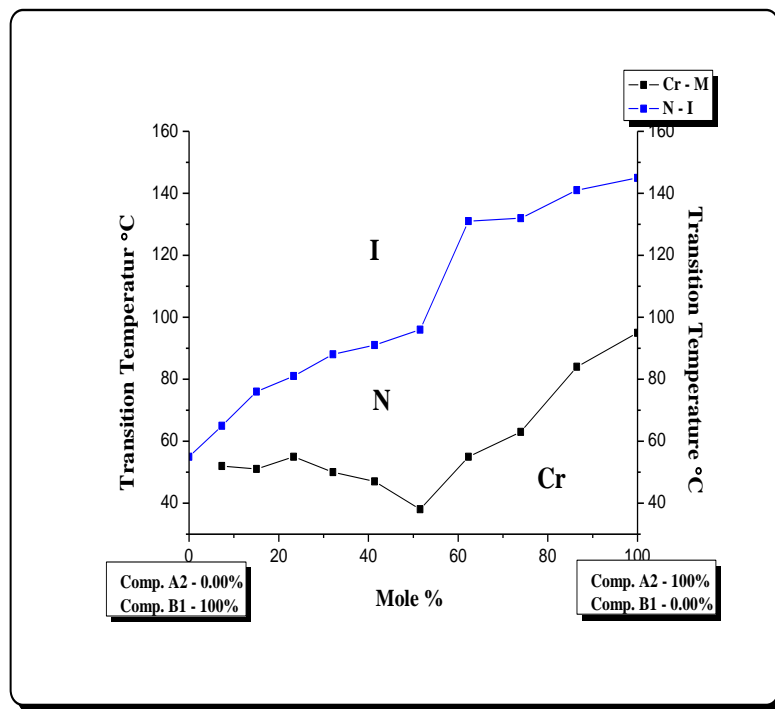
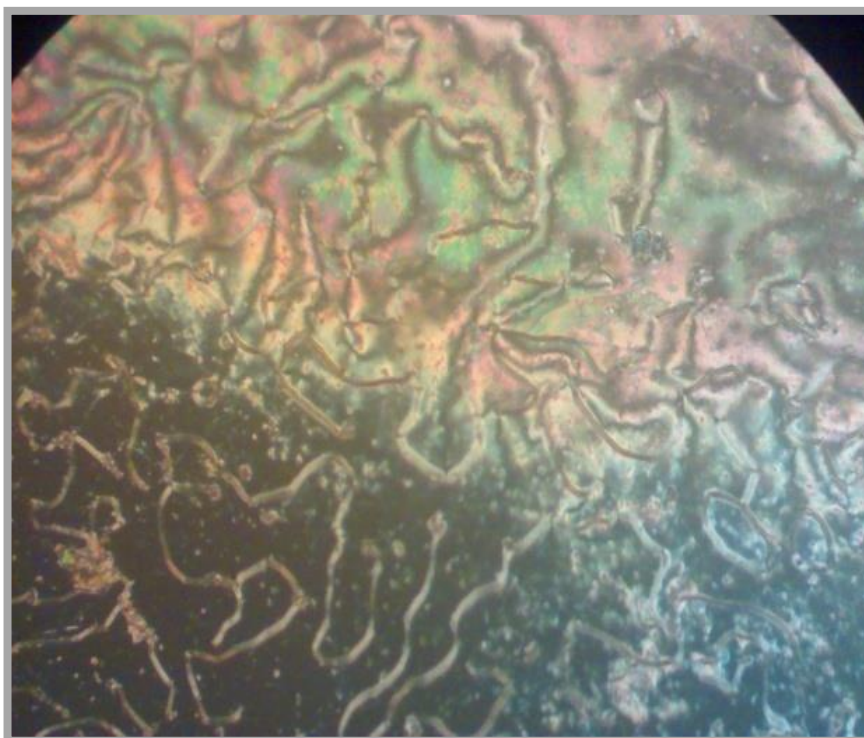


Figure 7.2: Phase diagram of Binary System II: HBMPAD (A2) + NPBB (B1)

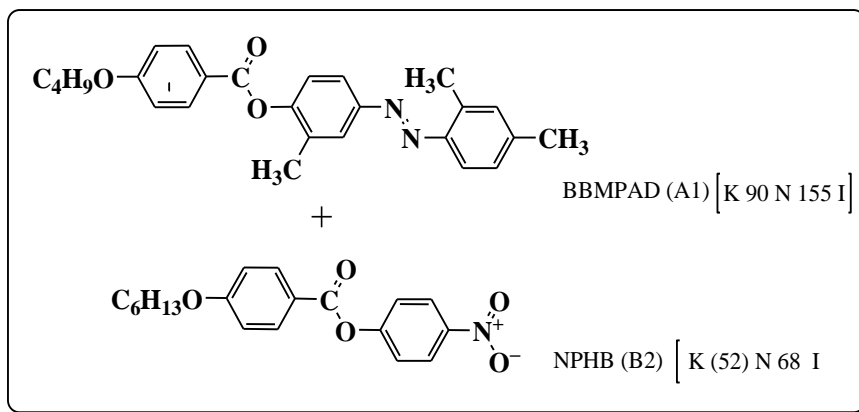
Polarizing optical microscopic image of Liquid Crystal

Polarizing optical microscopic image of binary system II at 62.30 mole%



Marble/Threaded texture of nematic phase of binary system II at 62.30 mole% at 102 °C on cooling.

7.3.3 Binary system III: BBMPAD (A1) + NPHB (B2)



In this system (Table 7.3, Figure 7.3) the ester component B2 is monotropic mesomorphic in nature (K (52) N 68 I), whereas the azo-ester mesogen A1 is enantiotropic mesomorphic in nature (K 90 N 155 I) showing nematic mesophase. The mesogenic characteristic commences in enantiotropic nematic form with the addition of as low as 8.38 mole % of A1 component and it continues to be exhibited till the last binary mixture studied. Binary system shows threaded/marble texture of nematic phase. The N-I curve shows deviation from linearity and highest mesophase range is obtained about of 57 °C at 55.29 mole% of A1 component. Eutectic point is obtained at 45.18 mole% of A1 component with eutectic temperature 47 °C.

Table 7.3: Binary System III: BBMPAD (A1) + NPHB (B2)

MOLE % OF A1	TRANSITION TEMPERATURE (NEMATIC °C)	TRANSITION TEMPERATURE (ISOTROPIC °C)
0.00	(52)	68
8.38	52	58
17.10	53	68
26.10	52	74
35.49	50	78
45.18	47	103
55.29	54	111
65.79	63	116
76.74	76	122
88.11	82	125
100.00	90	155

()* Value in the parenthesis indicates monotropy.

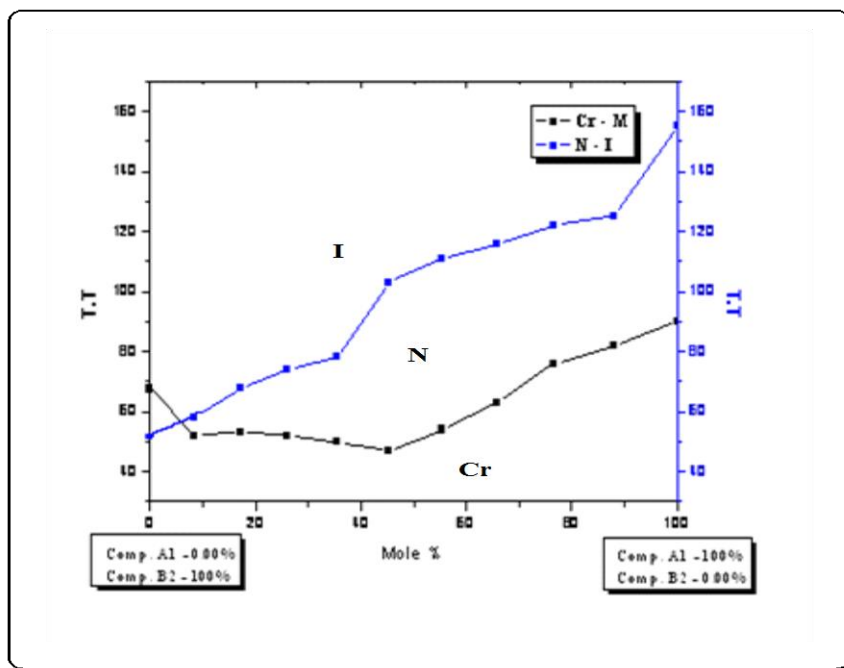
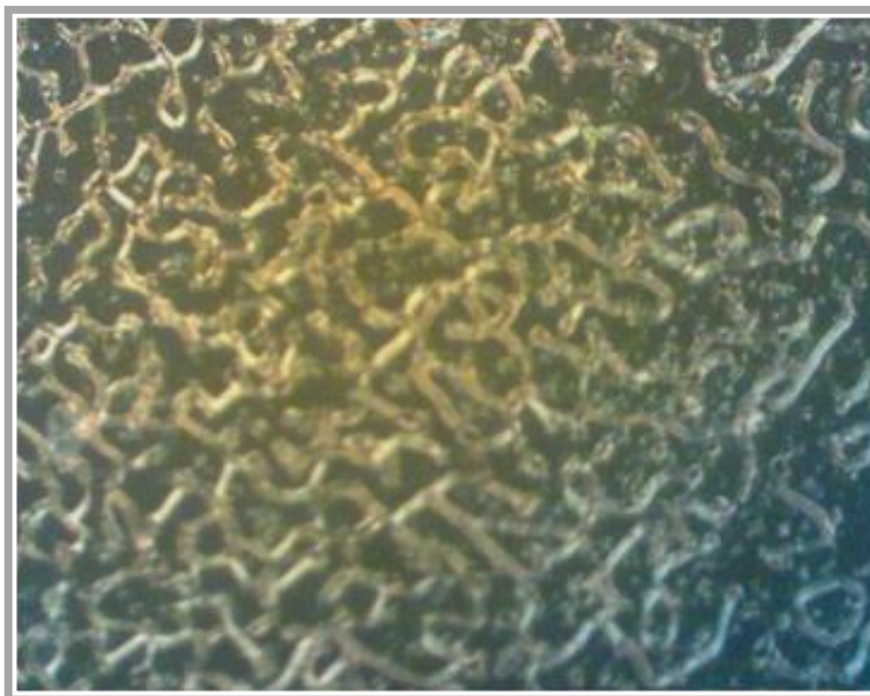


Figure 7.3: Phase diagram of Binary System III: BBMPAD (A1) + NPHB (B2)

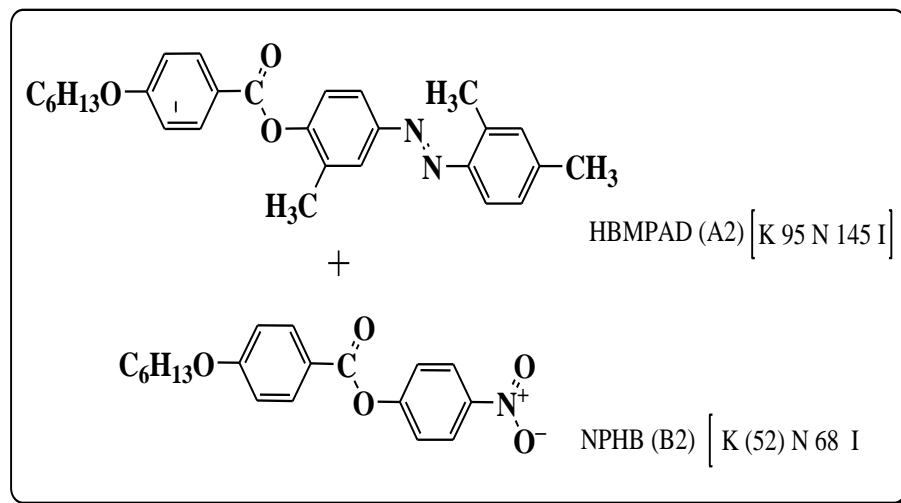
Polarizing optical microscopic image of Liquid Crystal

Polarizing optical microscopic image of binary system III at 45.18 mole%



Threaded texture of nematic phase of binary system III at 45.18 mole% at 78 °C on cooling.

7.3.4 Binary system IV: HBMPAD (A2) + NPHB (B2)



In this system (table 7.4, figure 7.4) the ester component B2 is monotropic nematogen (K (52) N 68 I), where as the azo mesogen A2 is enantiotropic nematogen (K 95 N 145 I). The mesogenic characteristic commences in enantiotropic nematic form with the addition of as low as 7.75 mole % of A2 component and it continues to be exhibited till the last binary mixture studied. Binary system shows threaded/marble texture of nematic phase. Here the eutectic point is sharp point at 53.17 mole% of A2; N-I curve shows deviation from linearity maximum mesophase range is obtained of 66 °C at eutectic point.

Table 7.4: Binary System-IV: HBMPAD (A2) + NPHB (B2)

MOLE %OF A2	TRANSITION TEMPERATURE (NEMATIC °C)	TRANSITION TEMPERATURE (ISOTROPIC °C)
0.00	(52)	68
7.75	52	63
15.92	52	73
24.50	54	85
33.55	52	88
43.10	46	94
53.17	43	109
63.87	53	114
75.18	65	121
87.21	84	128
100.00	95	145

()* Value in the parenthesis indicates monotropy.

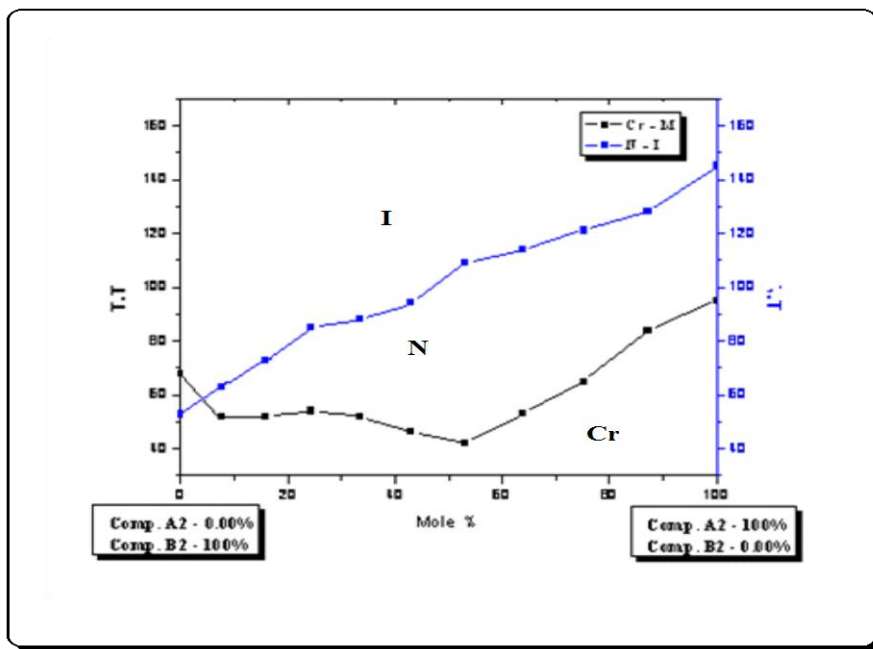
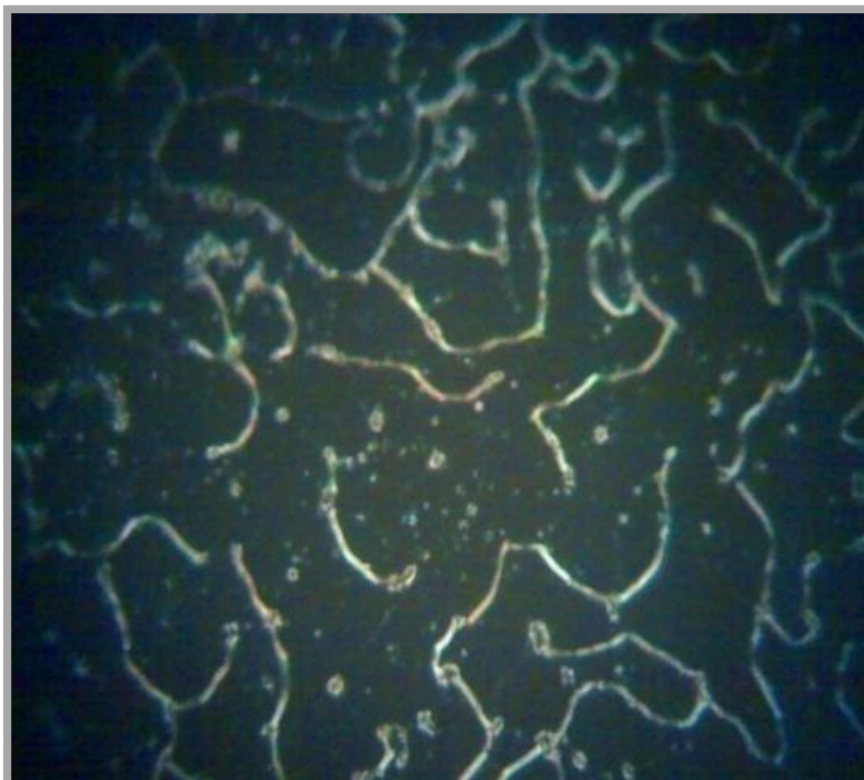


Figure 7.4: Phase diagram of Binary System IV: HBMPAD (A2) + NPHB (B2)

Polarizing optical microscopic image of Liquid Crystal

Polarizing optical microscopic image of binary system IV at 53.17 mole%



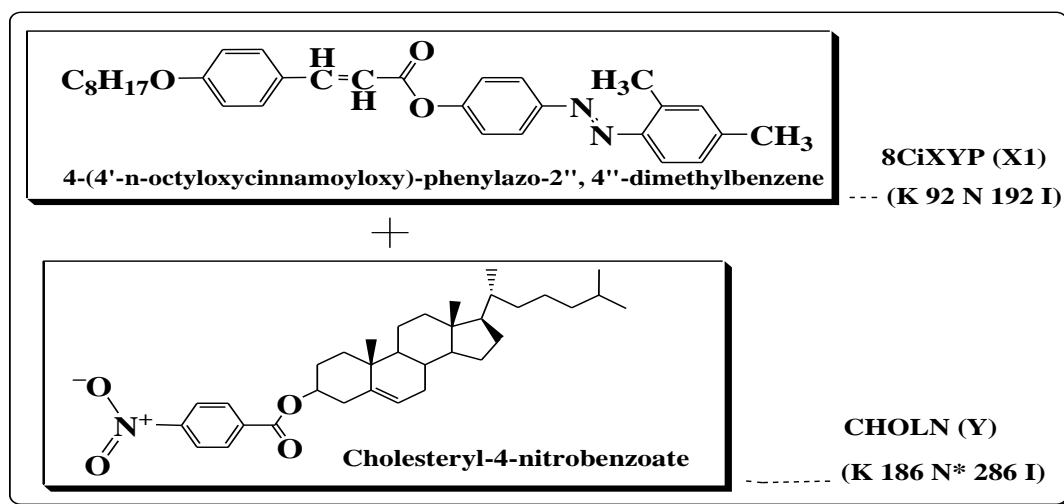
Threaded texture of nematic phase of binary system IV at 53.17 mole% at 97 °C on cooling.

7.3.5 Conclusion

In all binary systems, nematic mesophase emerges in enantiotropic nematic form with the addition of less than 9 mole % of azo-ester mesogenic components. In all the four binary systems N-I curve deviates from linearity. Some of the mixtures super cool below 35 °C which can be potential mixtures for optical display applications.

7.4 Type 2: Binary System [V to X]

7.4.1 Binary system V: 8CiXYP (X1) + CHOLN (Y)



In this system (table 7.5, figure 7.5), the azo-ester mesogen X1 is enantiotropic nematogen (K 92 N 199 I) and Component Y is cholesteric ester derivative nematogen (K 186 N* 286 I). The mesogenic characteristic commences in enantiotropic cholesteric nematic form with the addition of as low as 12.29 mole % of Y component and it continues to be exhibited till the last binary mixture studied. Binary system shows oily streaks texture of cholesteric nematic phase. Smectic mesophase emerges with the addition of 62.41 mole % of Y component, here the eutectic point is sharp point at 52.54 mole% of Y, N*-I curve shows deviation from linearity.

Table 7.5: Binary System-V: 8CiXYP (A2) + CHOLN (Y)

Mole % of Y	TRANSITION TEMPERATURE °C SmA*	TRANSITION TEMPERATURE °C N*	TRANSITION TEMPERATURE °C N	TRANSITION TEMPERATURE °C I
0	-	-	92	199
12.29	-	132	-	189
27.67	-	127	-	215
32.17	-	112	-	192
42.46	-	79	-	185
52.54	-	75	-	206
62.41	(68)	161	-	210
72.10	(71)	140	-	195
81.57	(83)	151	-	212
90.87	(70)	93	-	175
100	-	186	--	286

()* Values in parentheses indicate monotropic transitions.

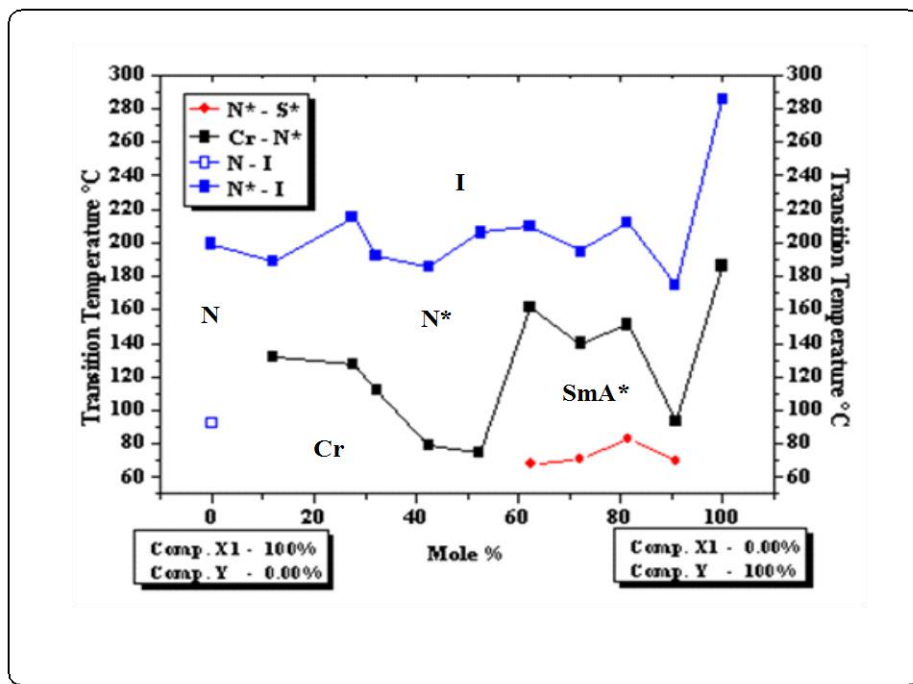
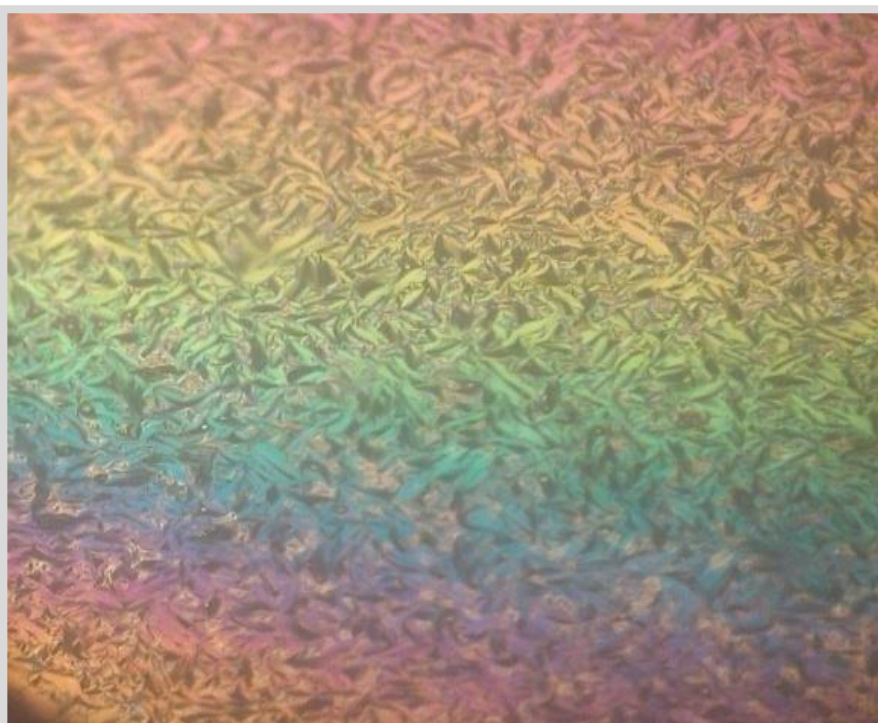


Figure 7.5: Phase diagram of Binary System V: 8CiXYP (X1) + CHOLN (Y)

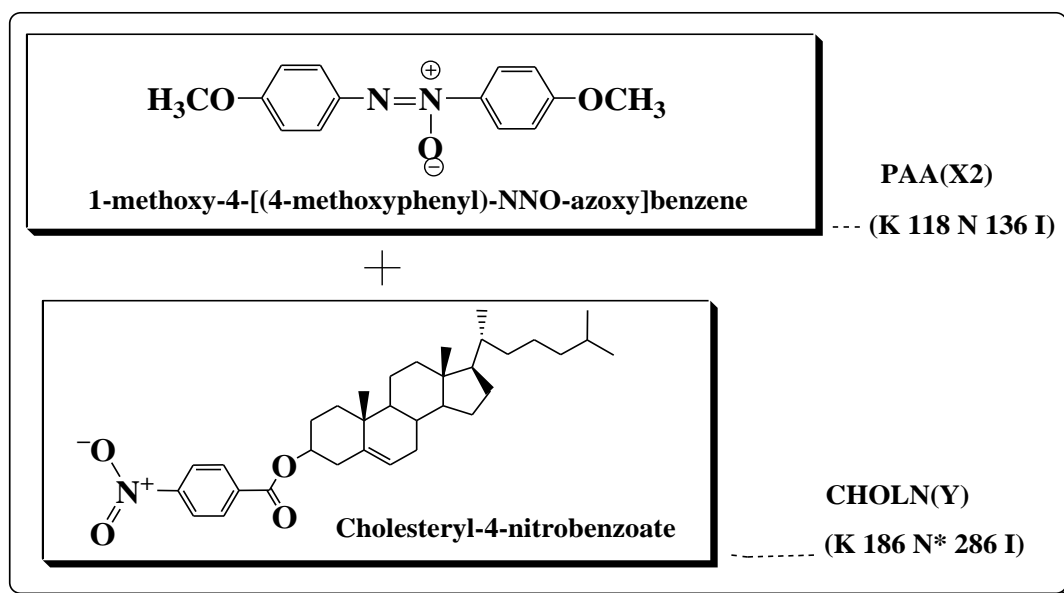
Polarizing optical microscopic image of Liquid Crystal

Polarizing optical microscopic image of binary system V at 72.10 mole%



Focal conic fan shaped texture of chiral smectic A* phase of binary system V at 72.10 mole% at 104 °C on cooling.

7.4.2 Binary system VI: PAA (X2) + CHOLN (Y)



This system (Table 7.6, Figure 7.6) consists of component X2 nematogen and component Y; cholesteric nematogen. The mesogenic characteristic commences in enantiotropic cholesteric nematic form with the addition of as low as 18.73 mole % of Y component and it continues to be exhibited till the last binary mixture studied. Binary system shows oily streaks texture of cholesteric nematic phase. Here the eutectic point is sharp point at 58.03 mole% of Y, N*-I curve shows deviation from linearity.

Table 7.6: Binary System-VI: PAA (X2) + CHOLN (Y)

Mole % of Y	TRANSITION TEMPERATURE °C N*	TRANSITION TEMPERATURE °C N	TRANSITION TEMPERATURE °C I
0	-	118	136
18.73	115	-	151
34.15	112	-	167
47.06	115	-	171
58.03	113	-	189
67.47	136	-	206
75.68	143	-	220
82.88	145	-	225
89.24	145	-	255
94.91	171	-	275
100	186	--	286

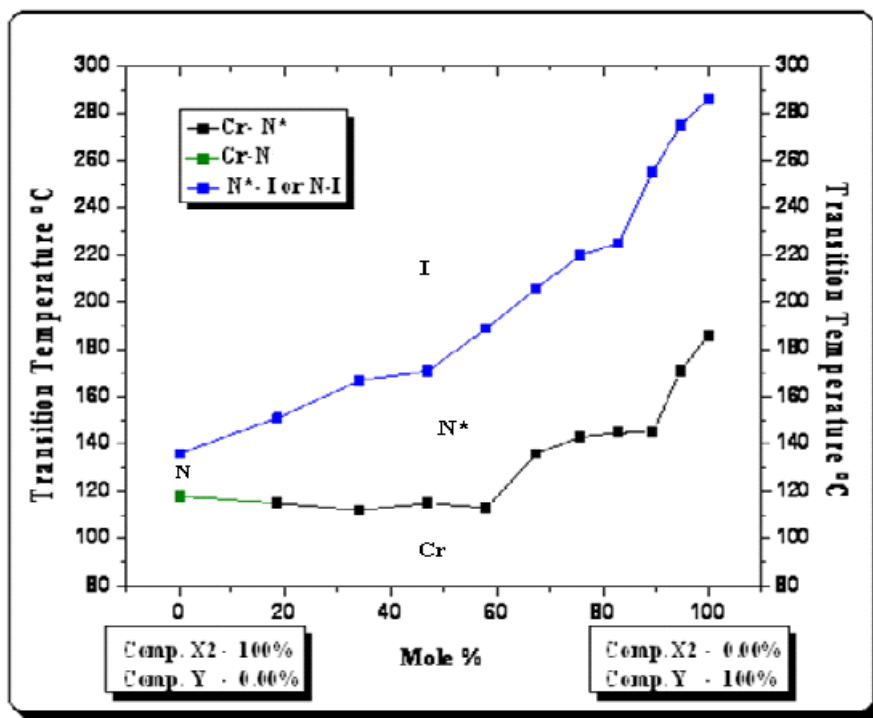
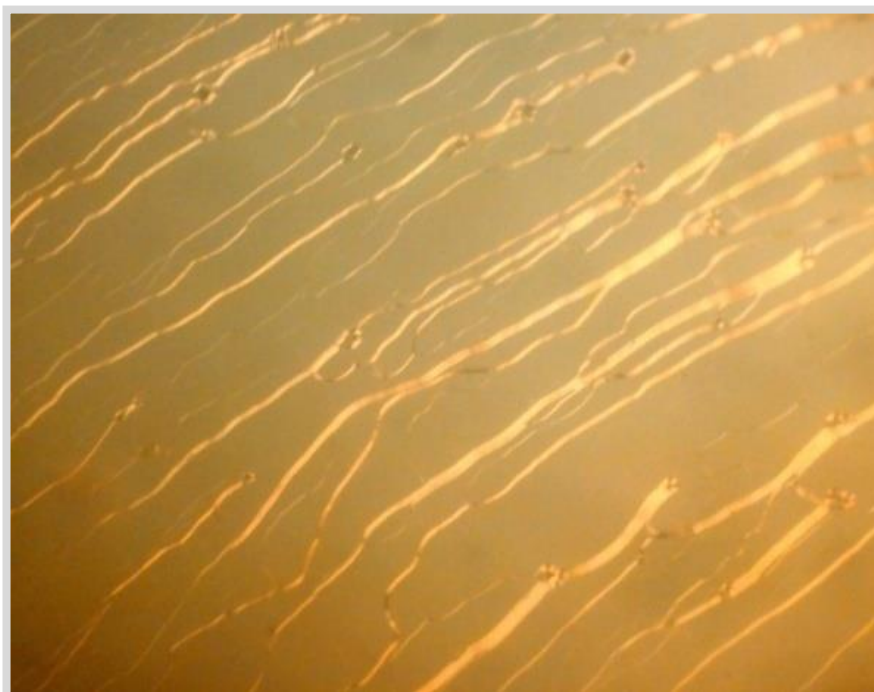


Figure 7.6: Phase diagram of Binary System VI: PAA (X2) + CHOLN (Y)

Polarizing optical microscopic image of Liquid Crystal

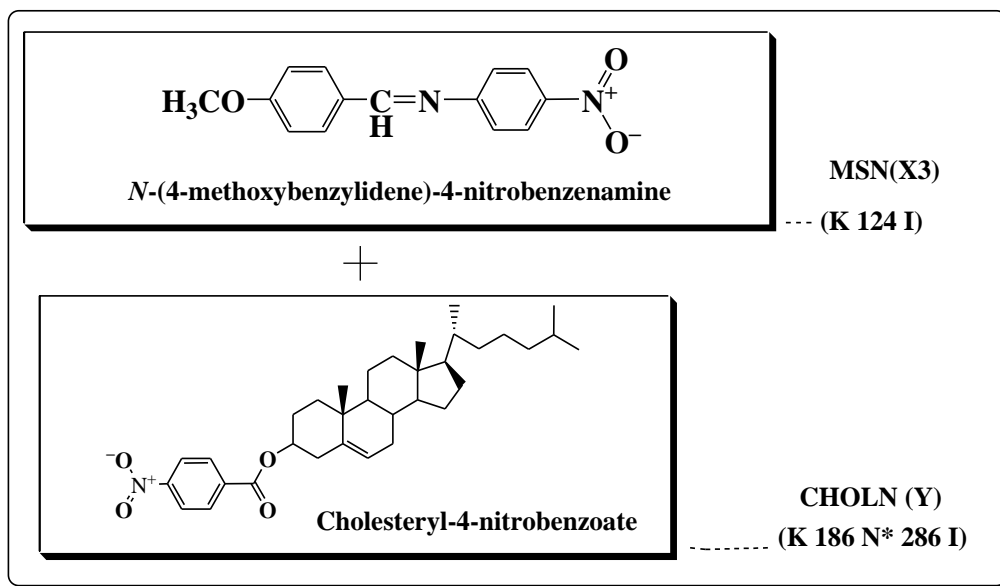
Polarizing optical microscopic image of binary system VI at 58.03 mole%



Oily streaks texture of chiral nematic N* phase of binary system VI at 58.03 mole% at 137 °C on cooling.

7.4.3

Binary system VII: MSN (X3) + CHOLN (Y)



In this system (table 7.7, figure 7.7) the ester component X1 is non-mesomorphic in nature (**K 124 I**); whereas the cholesteric ester component Y is mesomorphic in nature (**K 186 N* 286 I**) exhibiting nematic phase with oily streaks texture. The mesogenic characteristic commences in enantiotropic nematic form with the addition of as low as 58.22 mole % of Y component and it continues to be exhibited till the last binary mixture studied. The eutectic point is sharp and obtained at 123 °C with 89.31 mole % of Y, the N*- I curve shows deviation from linearity.

Table 7.7: Binary System-VII: MSN (X3) + CHOLN (Y)

Mole % of X3	TRANSITION TEMPERATURE °C N*	TRANSITION TEMPERATURE °C I
0	-	124
18.85	-	134
34.33	-	132
47.25	-	135
58.22	148	186
67.65	138	194
75.82	134	199
82.98	129	209
89.31	123	234
94.95	186	255
100	186	286

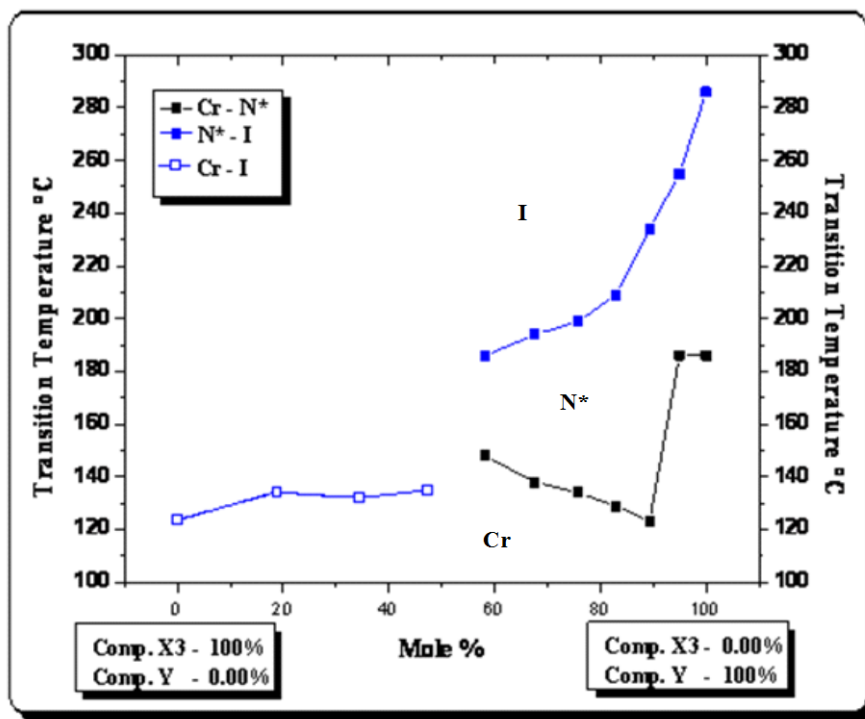
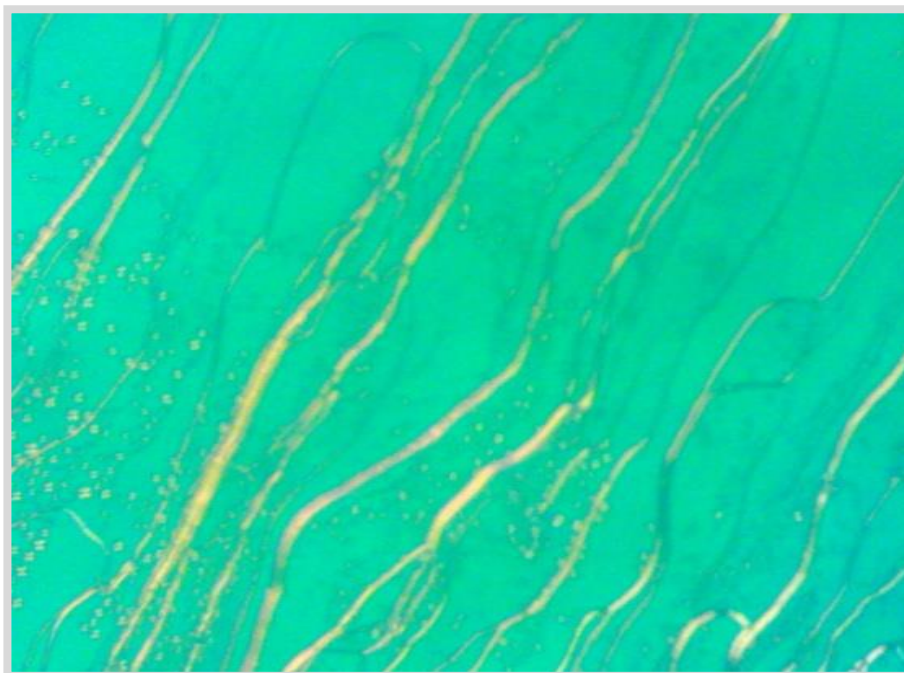


Figure 7.7: Phase diagram of Binary System VII: MSN (X3) + CHOLN (Y)

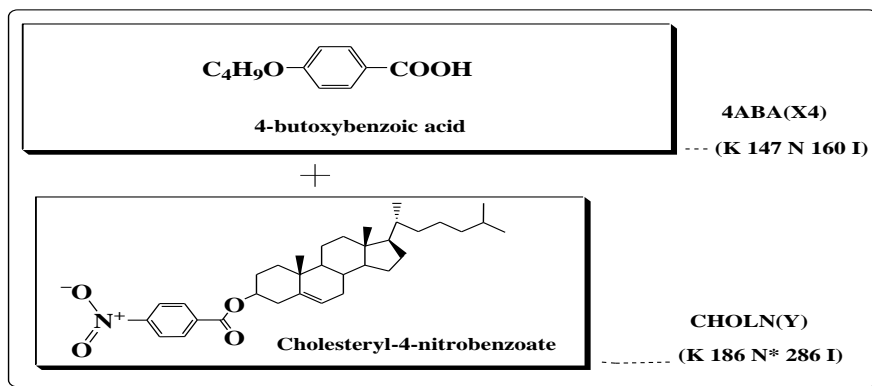
Polarizing optical microscopic image of Liquid Crystal

Polarizing optical microscopic image of binary system VII at 58.22 mole%



Oily streaks texture of chiral nematic N* phase of binary system VII at 58.22 mole% at 172 °C on cooling.

7.4.4 Binary system VIII: 4ABA (X4) + CHOLN (Y)



In this binary system (Table: 7.8, Figure: 7.8), 4-*n*-butoxybenzoic acid (K 147 N 160 I) component X4 is nematogen and cholesteryl-4-nitrobenzoate component Y is cholesteric nematogen (K 186 N* 286 I). Chiral mesophase in the form of Nematic phase N* induced with the addition of 23.47 mole % chiral dopant Y it continues to be exhibited till the last binary mixture studied. Last two mixtures of this binary system show chiral smectic mesophase alongwith chiral nematic phase. The eutectic point is sharp and is obtained at 86.57 mole% of Y with maximum mesophase range of 74 °C. The N* - I curve shows deviation from linearity and a very steep rise of 97 °C from 96.13 mole% of Y to 100 mole %, in other words the depression in last mix is of 97 °C. Chiral nematic mesophase shows oily steaks texture whereas chiral smectic mesophase of the system exhibits focal conic fan shaped texture of chiral smectic A* variety.

Table 7.8: Binary System-VIII: 4ABA (X4) + CHOLN (Y)

Mole % of Y	T. T. °C SmA*	T. T. °C N*	T. T. °C N	T. T. °C I
0.00	--	--	147	160
23.47	--	144	--	172
40.83	--	137	--	165
54.19	--	130	--	167
64.80	--	135	--	178
73.41	--	152	--	189
80.55	--	127	--	190
86.57	--	124	--	198
91.69	126	178	--	189
96.13	142	184	--	189
100.00	--	186	--	286

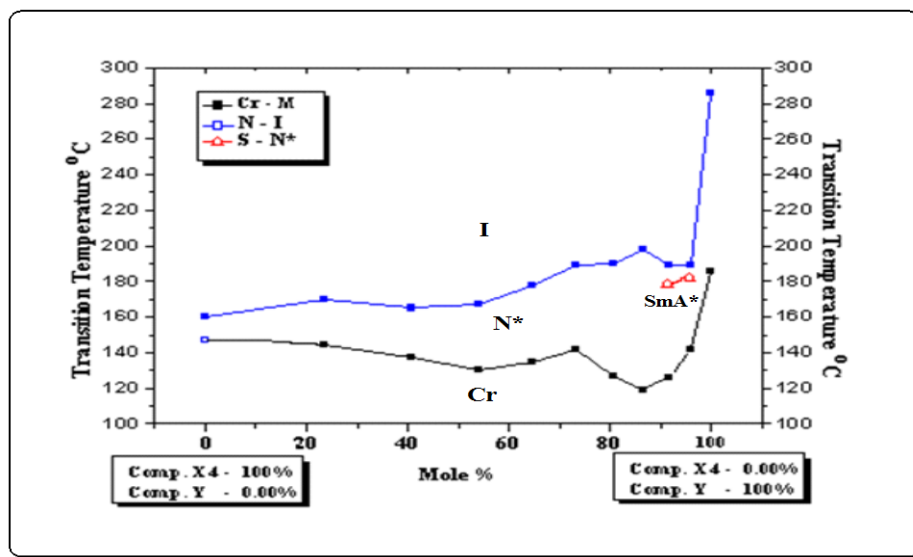


Figure 7.8: Phase diagram of Binary System VIII: ABA (X4) + CHOLN (Y)

Polarizing optical microscopic images of Liquid Crystals

Polarizing optical microscopic images of binary system VIII at 91.69 mole%



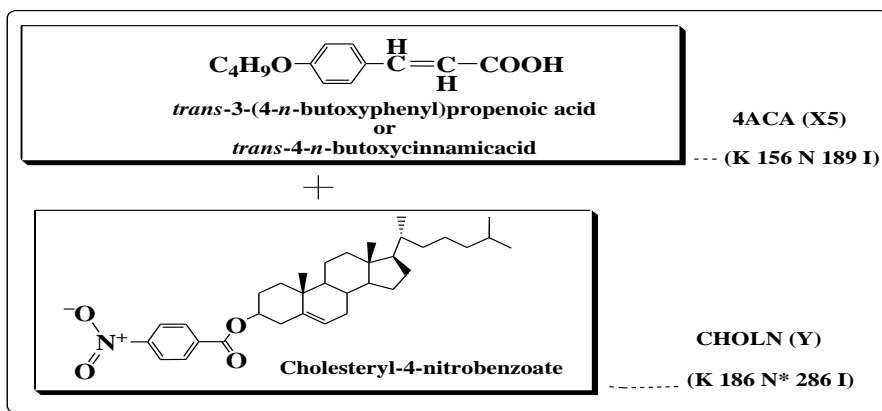
(a)

(b)

- (a) Focal conic fan shaped texture of chiral smectic A* phase of binary system VIII at 91.69 mole% 134 °C on cooling.
- (b) Fingerprint texture of chiral nematic N* phase of binary system VII at 91.69 mole% at 184 °C on cooling.

7.4.5

Binary system IX: 4ACA (X5) + CHOLN (Y)



In this binary system (Table: 7.8, Figure: 7.8), *trans*-4-*n*-butoxycinnamic acid or *trans*-3-(4-*n*-butoxyphenyl)-propenoic acid component X5 (K 156 N 189 I) and component Y is cholesteric nematogen (K 186 N* 286 I). Chiral mesophase in the form of nematic phase N* induced with the addition of 21.29 mole % chiral dopant Y, chiral smectic A* mesophase emerges with the addition of 37.84 mole % of Y continues upto the last mixture studied. Chiral smectic C mesophase commences in monotropic form, with the addition of 61.88 mole% of Y and continues till the addition of 85.04 mole% of Y. The N – I curve at N* – I curve at 21.29 mole % of Y and continues as SA* – I curve showing linear behavior. It is interesting to note that the last mixture with 95.63 mole% of Y shows 118 °C. The eutectic point with maximum mesophase range of 74 °C is obtained at 78.51 mole% of Y. Chiral smectic mesophase exhibits focal conic fan shaped texture of smectic A* whereas chiral smectic C* mesophase emerges with spiral texture of smectic C* variety.

Table 7.9: Binary System-IX: 4ACA (X4) + CHOLN (Y)

Mole % of Y	T. T. °C SmC*	T. T. °C SmA*	T. T. °C N*	T. T. °C N	T. T. °C I
0	-	-	-	156	189
21.29	-	-	126	-	174
37.84	-	132	-	-	206
51.06	-	132	-	-	203
61.88	(115)	135	-	-	195
70.89	(129)	159	-	-	200
78.51	(121)	126	-	-	200
85.04	(121)	136	-	-	189
90.60	-	135	-	-	178
95.63	-	142	-	-	168
100	-	-	186	--	286

(*) values in the parenthesis indicate monotropic transitions.

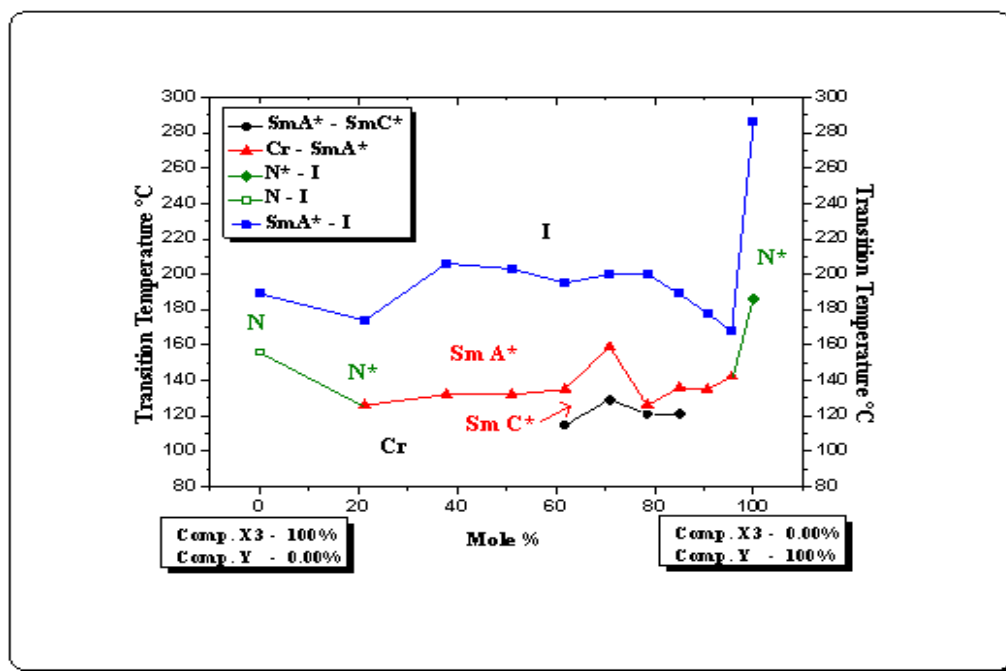
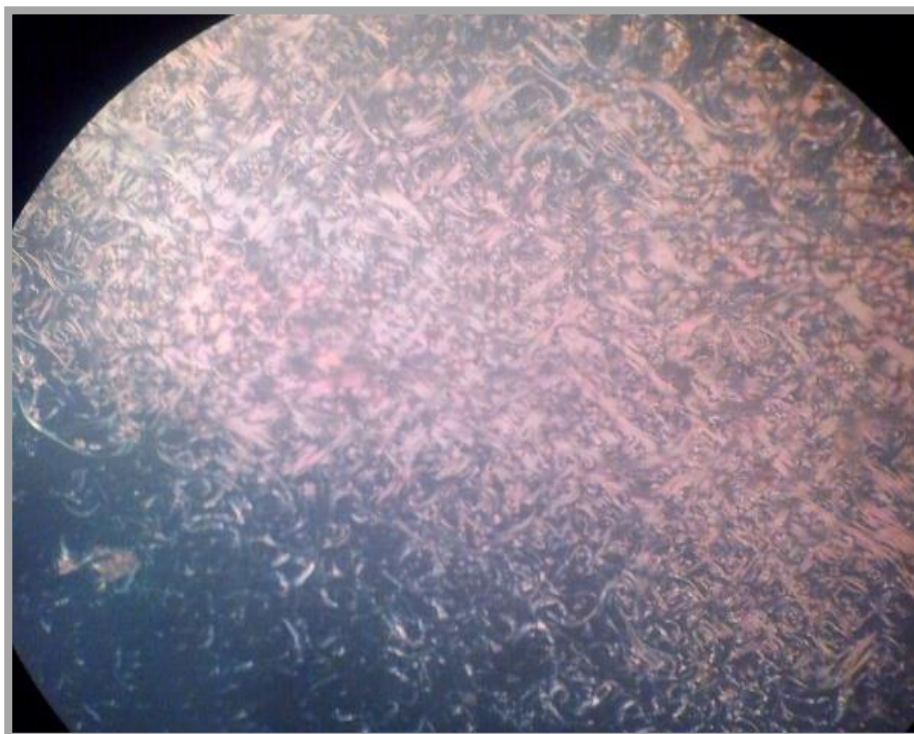


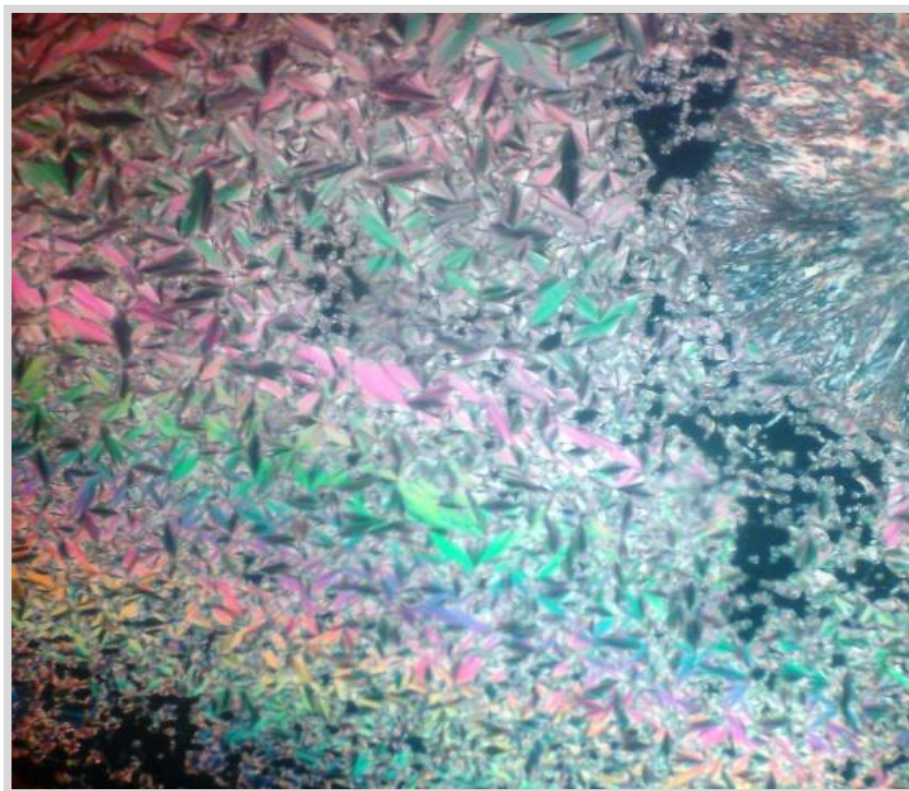
Figure 7.9: Phase diagram of Binary System IX: 4ACA (X5) + CHOLN (Y)

Polarizing optical microscopic images of Liquid Crystals

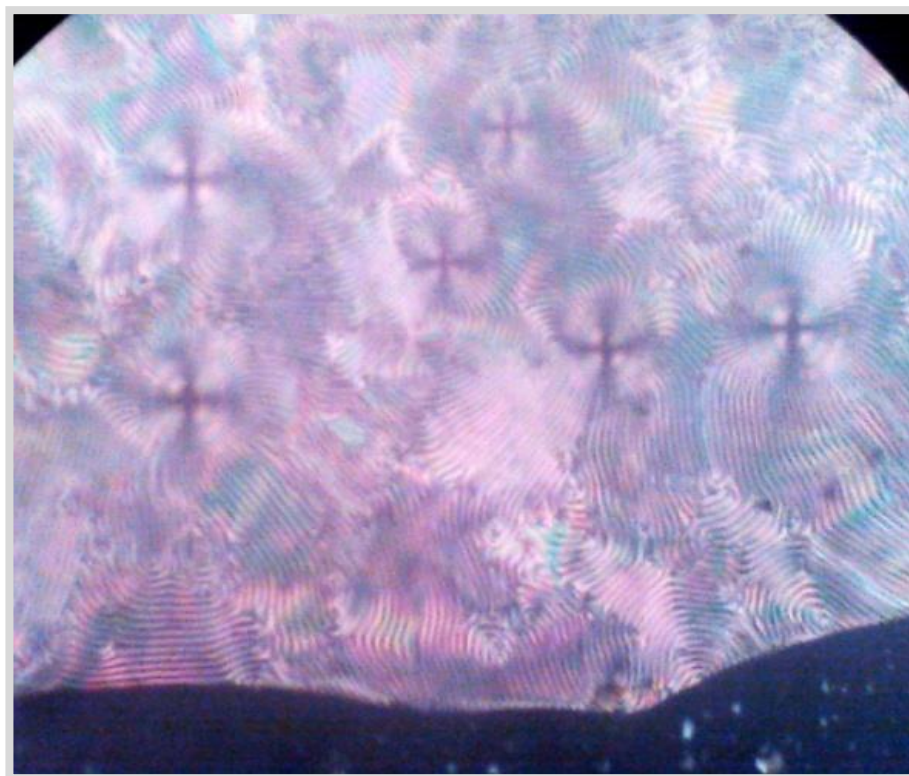
Polarizing optical microscopic images of binary system IX.



Spiral texture of chiral smectic C* phase at 78.51 mole% at 124 °C on cooling.



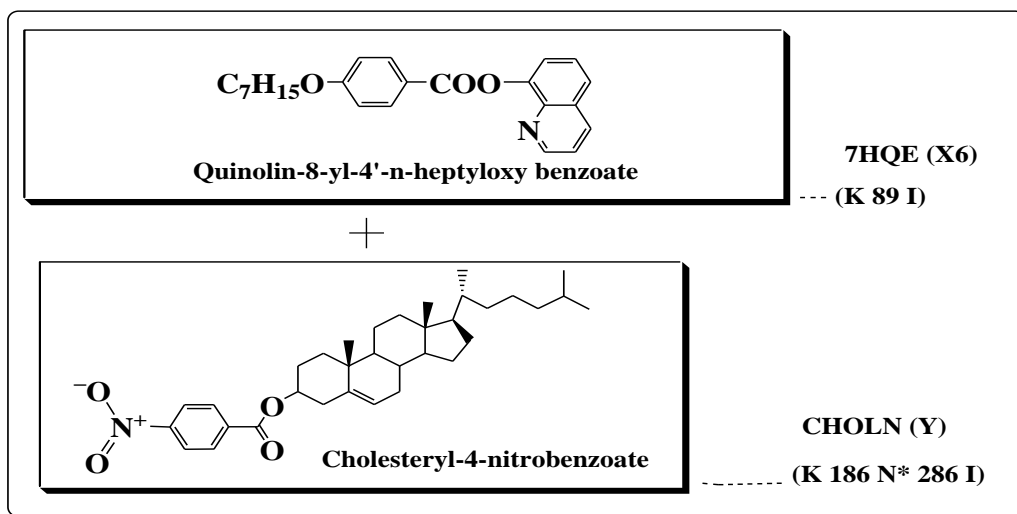
Focal conic fan shaped texture of chiral smectic A* phase at 37.84 mole% at 119 °C on cooling.



Fingerprint texture of chiral nematic N* phase at 21.29 mole% at 158 °C on cooling.

7.4.6

Binary system X: 7HQE (X6) + CHOLN (Y)



In this binary system (table 7.10, figure 7.10), the heterocyclic ester component X6 is non-mesomorphic in nature (**K 89 I**); whereas the cholesteric ester component Y is chiral mesomorphic in nature (**K 186 N* 286 I**). The mesogenic characteristic commences in enantiotropic chiral nematic N* form with the addition of 59.61 mole % of Y component and it continues to be exhibited till the last binary mixture studied. The eutectic point is obtained at 157 °C with 68.88 mole % of X6. The N* – I curve shows deviation from linearity; the maximum mesophase range of 31 °C is obtained at 92.99 mole % of Y. The last mixture with 92.99 mole% shows depression of 71 °C. Chiral nematic mesophase of the system exhibits oily streaks texture.

Table 7.10: Binary System-X: 7HQE (X6) + CHOLN (Y)

MOLE % OF Y	T. T. °C N*	T. T. °C I
0.00	-	89
14.08	-	148
26.95	-	147
38.74	-	157
49.59	-	172
59.61	178	202
68.88	157	184
77.51	180	204
85.51	181	205
92.99	184	215
100.00	186	286

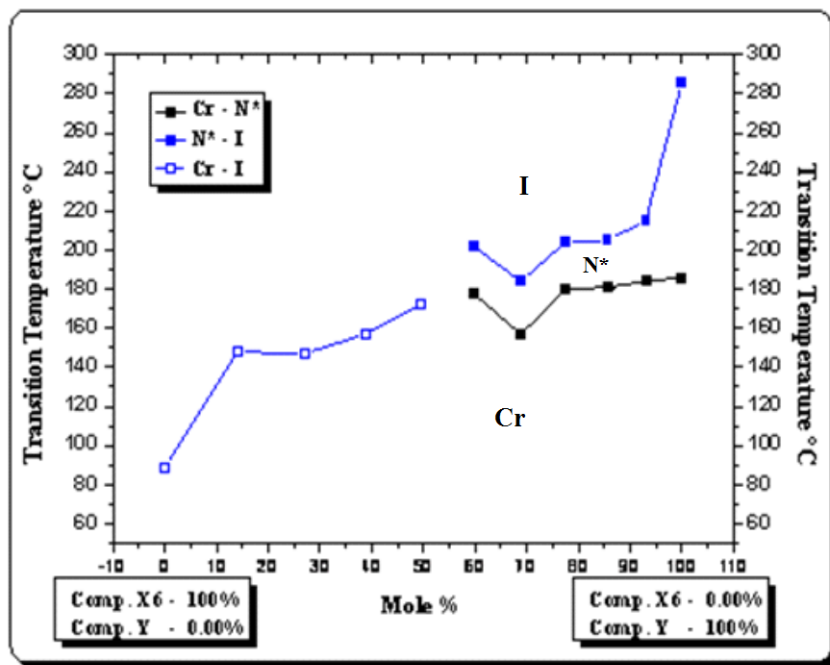
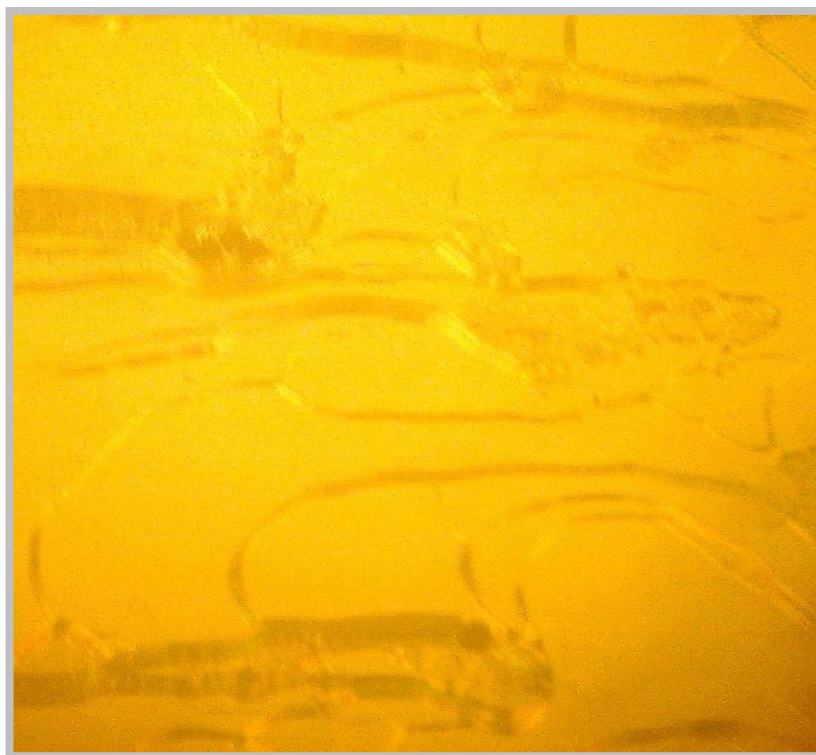


Figure 7.10: Phase diagram of Binary System X: 7HQE (X6) + CHOLN (Y)

Polarizing optical microscopic images of Liquid Crystals

Polarizing optical microscopic images of binary system X at 68.88 mole%



Oil streaks texture of chiral nematic N* phase at 68.88 mole% at 169 °C on cooling.

7.4.7 Conclusion

In all binary systems, cholesteric mesophase emerges in enantiotropic nematic form with the addition of less than 24 mole % of cholesteric components. In all the six binary systems $N^* - I$ curve deviates from linearity.

The above study of binary mixtures of chiral dopant in to different achiral components reveals that the chiral dopant component induces chiral N^* mesophase in the binary systems; in some mixtures chiral smectic, mixes with the achiral different nematogens. smectogenic behavior arises, this can be due to chirality transfer via core-core interaction (502) it seems that the molecules (X1, X4 and X5) are right to be set in to the crystal lattice of chiral dopant Y to be exhibits smectogenic layer formations in the form of smectic C^* or smectic A^* variety.